Polymer(Korea) Vol. 21, No. 4, pp 689-700(1997)

Micromechanics 시험법과 Acoustic Emission을 이용한 Brittle/Ductile Dual Matrix 복합재료의 계면물성 고찰

박 종 만† · 이 상 일

경상대학교 고분자공학과, 항공기부품기술 연구센타

(1997년 3월 19일 접수)

Interfacial Aspects of Fiber Reinforced Brittle/Ductile Dual Matrix Composites using Micromechanics Techniques and Acoustic Emission

Joung-Man Park† and Sang-Il Lee

Department of Polymer Science & Engineering, Eng. & Research Center for Aircraft Part Technology, Gyeongsang National University, Chinju 660-701, Korea

(Received March 19, 1997)

요 약: 유리섬유 강화된 취성의 불포화폴리에스터/변성된 에폭시 복합재료의 계면결합과 미세파괴 형태에 대한 연구가 micromechanics 시험법과 acoustic emission (AE)를 통하여 조사되었다. 여러 silane coupling agents를 이용하여 상대적인 계면결합력과 미세파괴 형태를 관찰하였다. Dry와 wet 두 상태에서, 취성인 기지 부분에서 cracking수가 증가할수록, 더 큰 계면결합력을 보여주었다. 계면결합력 증가는 다른 두 계면에서의 화학적, 또는 수소결합력에 기인한다고 여겨진다. Microdroplet와 fragmentation 시험법들과 model system간에 적절한 상호관련이 이루어졌으며, AE 변수와 관련하여 행해졌다. AE의 검사는 주로 세 groups의 발생을 보여주었다. 첫째는 주로 취성기지의 cracking으로부터 발생하며, 둘째와 셋째는 섬유의 파단과 debonding 등을 포함하는 복잡한 연성기지로부터 각각 발생하였다. Micromechanics 시험법과 AE를 이용한 이중 기지 시편은 계면결합력과 미세파괴 연구에 신뢰성있는 정보를 제공해 줄 수 있을 것이다.

ABSTRACT: Interfacial bonding and microfailure modes of glass fiber reinforced brittle unsaturated polyester/modified epoxy composites were investigated via micromechanics techniques and acoustic emission (AE). Various silane coupling agents were used to observe the comparative interfacial bonding. In the brittle matrix layer, the more the numbers of cracking increased, the higher the interfacial bonding was improved under both dry and wet conditions. This might be due to the chemical and hydrogen bondings in two interphases. A reasonable correlation among microdroplet, fragmentation tests and model system was found. This can be performed by associating AE parameters. AE data showed the sequential occurrence of main three groups of AE. The first group was originated mainly from brittle matrix cracking. The second and the third resulted from the fiber breakages and complex ductile matrix cracking including debonding, respectively. The micromechanical tests for dual matrix specimens provided more reliable information on the interfacial adhesion and charaterized microfailure modes when combining AE technique.

Keywords: *dual matrix composites, fragmentation test, microdroplet test, interfacial shear strength, acoustic emission.*

INTRODUCTION

Interfacial shear strength (IFSS) between fiber and matrix plays an important role in controlling composite properties. A relatively strong interfacial bond is needed for an efficient transfer of the applied load. In case of weak interfacial bond, fracture toughness can be improved by debonding and crack blunting mechanisms occurring at the interphase. It is necessary that the interfacial bond should be determined via an optimization in accordance with the ultimate purpose. The IFSS in fiber reinforced composites can be improved by an introduction of chemical functional groups by oxidation, plasma treatment and commercial coupling agents coating of the fiber surface.

Measuring the IFSS between fiber and matrix requires special micromechanical techniques. Some of conventional techniques for the IFSS include the single fiber microdroplet test which is also called as the single fiber pull-out test,[1,2] the fragmentation test which is called as the single fiber composite test[3-5] and the microindentation method.[6]

Among them, considerable attention was drawn to the single fiber pull-out test in measuring the IFSS, since this technique showed distinct advantage over the others, i.e., a direct measure of the adhesive bond between the fiber and matrix, no limitation in the properties of the fiber and matrix. On the other hand, in the case of fragmentation test, the failure strain of the matrix needs to be more than three or four times the failure strain of the fiber to meet the need of achieving a saturated fragmentation state. In practice, however, both techniques are complementary each other.

The dual matrix composite[7-9] consists of a single fiber, brittle inner matrix layer and ductile outer matrix resulting in many fragments of the embedded fiber and coating layer while subjecting to the tensile load. The main idea of the new specimen design is to allow the specimen to undergo the necessary elongation without premature failure of the matrix.

The specimen of modified fragmentation test was prepared by two processes. One is to coat on the fiber surface with brittle matrix resin, and the other is to embed the coated fiber into a more ductile resin which acts as a support to maintain the specimen integrity. Thin layer coating is made on the single fiber with brittle matrix. After curing, the fiber/brittle matrix is molded into the same dogbone specimens as before with an excess of the ductile matrix.[8] When such a 'bimatrix' specimen is loaded in tension, each fiber rupture induces a fracture of the brittle layer by crack propagation. However, this 'penny shape crack' is now stopped by the tougher support at the second interface, thus preventing the complete fracture of the specimen.

Acoustic emission (AE) technique has been considered rapidly as a highly reliable way of detecting the active microscopic failure events in composite materials. There is now increasing interest in the use of AE techniques for monitoring failure processes in composite materials.[10,11] When a composite material consisting of fiber and a polymeric matrix is subjected to external load, acoustic emission may occur from : fiber fracture, matrix cracking, and debonding at the fiber-matrix interface. It is, therefore, important to identify the source of emission in order to obtain information about the fracture mechanism in the fiber reinforced composites, and is possible to forecast their imminent fracture. There have been many studies[12,13] which attempt to correlate the AE activity with fiber fracture for a composite containing brittle fibers in a polymer matrix. The energy released by fiber frac-

ture could be much greater than that associated with debonding or matrix cracking. In particular, AE is useful for opaque matrix composites being difficult to monitor optically.

In this work, the IFSS and microfailure modes of fiber reinforced brittle/ductile dual matrix composites were evaluated using fragmentation, microdroplet methods and AE technique. The effect of the surface treatment using various coupling agents on the interfacial adhesion was also studied in detail.

EXPERIMENTAL

Fiber. Two kinds of E-glass fibers with diameters of 14.7 μm and 30.3 μm were used without sizing. E-glass fiber was supplied from Dow Corning Co. The elastic moduli of glass fibers were 74.3 GPa for 14.7 μm and 58.6 GPa for 30.3 μm, respectively. The average density was 2.55 g/cm^3, and the tensile strength of the glass fibers was measured before fabricating composites.

Coupling Agents. Various silanes including vinylbenzylamino- (VBAS) and methacryloxy-functional groups were used as coupling agents. Silane coupling agents were diluted to the required concentration in aqueous solutions on glass fiber surface. Although a polymeric solution is not a coupling agent, it was used for the purpose of the improvement of the IFSS by increasing wettability.

Polymer Matrix. The brittle matrix in dual matrix specimen and microdroplet in the microdroplet test were prepared with unsaturated polyester (R-585). Benzoylperoxide (BPO) at high temperature and methylethylketone-peroxide (MEKPO) at room temperature were individually used as curing agents. The curing condition of high temperature is for 30 min at 85 ℃, and at room temperature (25 ℃) for 3 days. For outer matrix of dual matrix specimen, the ductile matrix was prepared with epoxy resin Epon 828, which is based on diglycidylether of bisphenol-A (DGEBA). Jeffamine D400 and D2000 were used as curing agents. Flexibility of the specimens was controlled by changing the relative proportions of D400 versus D2000 in the curing mixture for ductile matrix. It was precured for 2 hrs at 80 ℃ and then postcured for 1 hr at 120 ℃.

Single Fiber Strength Measurement and Surface Treatment. About fifty specimens in the each gauge length were tested. The gauge lengths of testing specimens were 2, 5, 10, 20 and 100 mm. Test specimens were made by centering a single glass fiber on the middle of paper frame with each gauge length, then adhering the fiber using epoxy adhesives. Coupling agent was diluted in chosen solvent for 3 hrs. The glass fiber was coated individually in a steel frame to ensure uniform coating on the fiber surface and to avoid the complications of neighboring fiber interactions in a tow.

Preparation of Specimens and Microdroplet Test. For the four glass fibers fixed at regular distances in steel frame, microdroplets were formed on each fiber with a specially designed micro-needle. The sizes of microdroplets were measured individually using optical microscope and the distribution of microdroplets were in the range of 50 to 700 μm. The numbers of microdroplet were about 50-60 EA. The shear force at the interface was developed with applying the load. Microdroplet specimen was fixed by the microvise using the micrometer. The IFSS (τ) was calculated from the measured pull-out force using following expression:

$$\tau = (F_d/\pi D_f L) \quad (1)$$

where D_f and L are fiber diameter and length of fiber embedded in the resin, respectively. It is

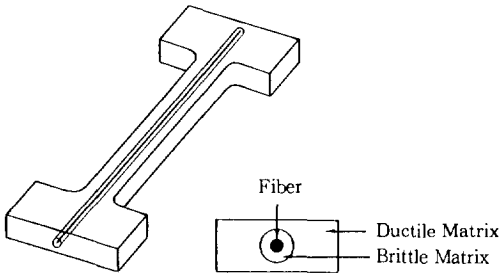

Figure 1. Dimension of dogbone-shaped dual matrices specimen for modified fragmentation test.

assumed that the linear relationship between pull-out force and embedded length of fiber. A relatively large scatter in the test data was observed mainly due to the testing parameters such as the position of the microdrop in the loading fixture.

Preparation of Dual Matrix Composites and Fragmentation Test. The glass fibers fixed in the steel frame were coated with unsaturated polyester. The average thickness of brittle layers were 80 to 100 μm (Fig. 1). This brittle layer again was embedded by the ductile epoxy in a dogbone mold. The modified fragmentation test was carried out to measure the number of brittle matrix fragments and to observe failure modes under specially designed strain machine. Load was applied until no further increase of matrix fragments was observed. The saturated numbers of brittle matrix crackings obtained from at least six specimens were averaged for each for statistical analysis. Fig. 2 shows the schematic plot of stress profiles in brittle matrix (σ_m) and fiber (σ_f). For the effect of moisture exposure on the interfacial adhesion, specimens were immersed in distilled water at boiling temperature for 2.5 hrs. After equilibration of the specimens for 1 hr at room temperature, then the number of brittle fragments was measured and microfailure modes were observed in the same way.

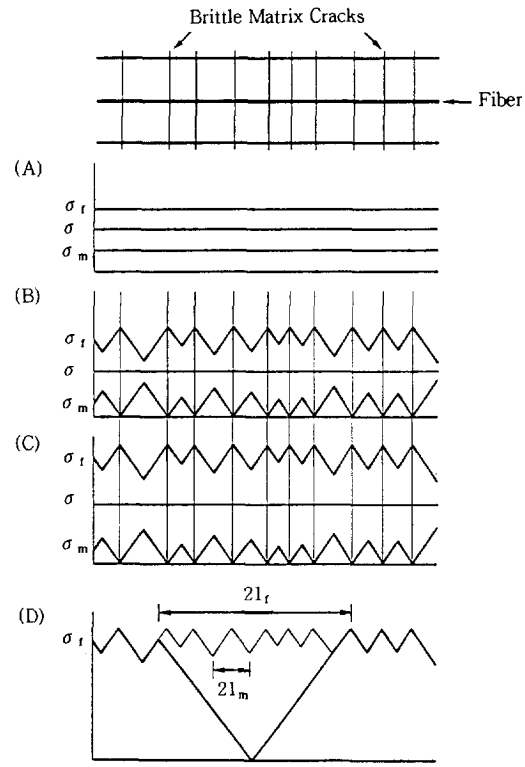

Figure 2. Schematic plot of stress in brittle matrix (σ_m) and fiber (σ_f) : (A) Just prior to matrix cracking, (B) just after matrix cracking at applied stress σ_{mc} ; (C) under further loading, $\sigma > \sigma_{mc}$,(D) fiber stress after a single break.

Measurement of Acoustic Emission (AE). AE sensor was attached to the center of the modified fragmentation specimen. AE signals were detected by a wideband type sensor with maximum sensitivity of -60 dB at 550 KHz. The sensor output was amplified by 60 dB at preamplifier then fed into an AE signal processing unit. Two AE parameters, peak amplitude and energy, were investigated for the time and the distribution analysis. Waveform analysis was carried out in the real time acquisition using digital oscilloscope (Fig. 3). Spectrum analysis of waveforms by fast Fourier transform (FFT) was used to analyze the characteristic frequency peaks.

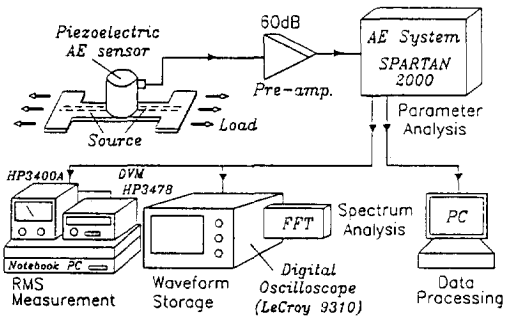

Figure 3. Schematic illustration of AE system.

Table 1. Tensile Strength and Elongation of Glass Fiber with Various Gauge Lengths

gauge length (mm)	No. of specimen (EA)	diameter (μm)	tensile strength (MPa)	elongation (%)
2	38	14.7 (0.5)*	2338 (481)	7.7 (2.4)
5	40	14.4 (0.7)	1939 (360)	3.4 (1.2)
10	42	14.3 (0.6)	1774 (384)	3.2 (0.8)
20	41	14.4 (0.8)	1485 (377)	2.2 (0.6)
100	39	14.6 (0.4)	1022 (268)	1.2 (0.4)

* Standard deviation.

RESULTS AND DISCUSSION

Statistical Analysis of Tensile Strength of Fiber. Table 1 showed the tensile strength and elongation of single glass fiber depending on various gauge lengths. As the gauge length increases, tensile strength and elongation decrease. It was considered due to the existence of defects and heterogeneous distribution of flaws on the fiber surfaces or internally existed flaws. In Fig. 4, the glass fiber coated with amino-silane showed a higher tensile strength and elongation values than the uncoated ones. This might be due to the surface flaw healing effect by coated layer. Tensile strength of glass fiber decreased at higher concentration more than 2 wt% probably because of the stress concentration at lump-shaped coating.

Interfacial Aspects by the Microdroplet and Modified Fragmentation Tests. Fig. 5 showed the embedded length versus pull-out force in the microdroplet test for both the VBAS treated and the untreated ones. VBAS treated specimens exhibited a higher pull-out force at same embedded length than the untreated one. The higher the slope is, the higher the IFSS exhibits. Improvement of the interfacial adhesion is due to chemical or physical bonding between two interphases in the composites. For interphase I between the fiber surface and the silane, there can be the siloxane bonding (Si-O-Si) between an hydroxyl group in glass fiber surface and silanol group in silane. For interphase II between silane and matrix, there can be a secondary H-bonding, covalent bonding and physical adhesion by interdiffusion between polymer matrix and silane. A typical pulled-out fiber from brittle unsaturated matrix after the microdroplet testing is shown in Fig. 6.

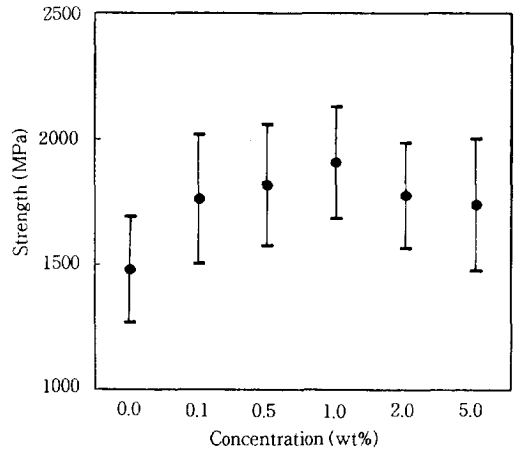

Figure 4. Tensile strength of glass fiber with diameter of 30.0 μm as a function of concentration of amino-silane coupling agent.

For uniform silane coating on a fiber surface, the silane concentration needed to be optimized. Surface morphology of fiber with coupling agent demonstrated that 0.5 wt% amino-silane solution was better than 5 wt% in the light of uni-

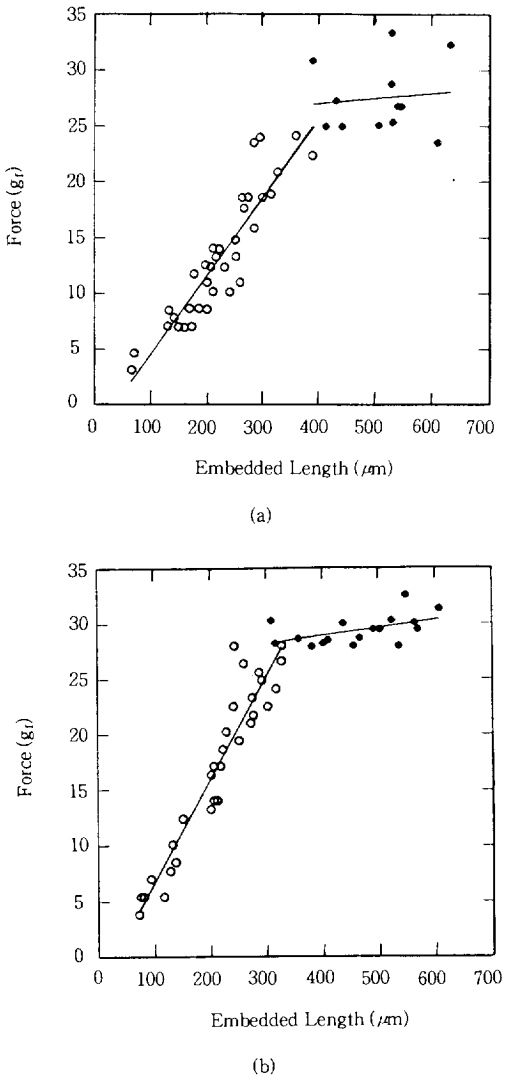

Figure 5. Pull-out force versus embedded length curve in the microdroplet test : (a) The untreated and (b) the VBAS 0.5 wt% treated.

formity (Fig. 7). An uneven fiber surface at more than 5 wt% silane concentration could cause weak boundary layer while combining with unsaturated polyester matrix.

The effect of coupling agent on the IFSS and its improvements in the microdroplet test is given in Table 2. Polymeric coating yielded the highest improvement compared to other coupling agents because of the improved compatibility and wettability for the same kind of resin. VBAS also showed comparably high improvement. The effect of various experimental conditions such as pot time, diameter, and different resins on the IFSS is shown in Table 3. The short pot time resulted from a low viscosity providing good wettability. The IFSS was higher in short pot time case than the long stored case which yielded a poor wetting. Similar IFSS value was obtained in two glass fibers with different diameters because of the same chemical composition. The brittle matrix fracture mode in the dual matrix composites was shown in Fig. 8. The treated with VBAS showed the better stress transfer through brittle matrix to fiber, and more brittle matrix fragmentations compared to the untreated one. The number of brittle matrix fragments under dry and wet conditions with various coupling agents were summarized in Fig. 9. The treated cases exhibited higher increment in the number of fragmentation under both dry and wet conditions. Under wet condition, the IFSS decreased dramatically due to plasticized water molecules

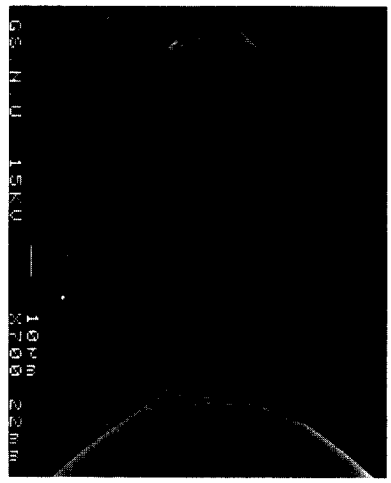

Figure 6. Typical failure mode of glass/unsaturated polyester microdroplet specimen after pulling-out.

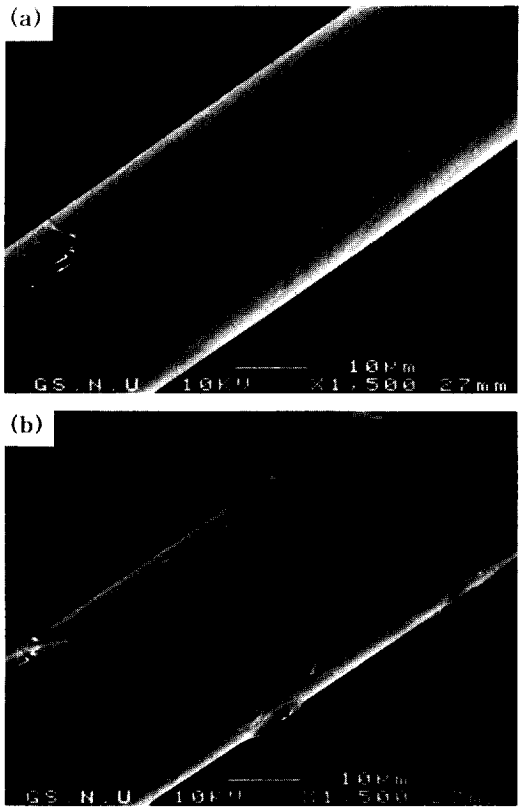

Figure 7. SEM photographs of glass fiber surfaces : (a) VBAS treated on the glass fiber (0.5 wt%, 1 min) and (b) silane treated on the glass fiber (5 wt%, 1 min).

Table 2. The IFSS and Their Improvement % with Various Coupling Agents in the Mcrodroplet Test

curing agents	IFSS (MPa)	improvements (%)
untreated	12.4 (2.5)*	–
UP coating[a]	16.8 (3.0)	35.9
VBAS[b]	15.1 (3.2)	22.0
A-174[c]	14.6 (2.7)	17.5
APS[d]	13.4 (1.6)	8.6
LiCA 38J[e]	12.8 (1.7)	3.0

* Standard deviation.
* Optimized condition : 85 ℃ for 30 min.
[a] Unsaturated polyester coating : Up 10 wt% styrene solution.
[b] VBAS : 3[2(vinyl benzyl amino) ethyl amino] propyl trimethoxy silane; 0.5 wt% MtOH solution.
[c] A-174 : Methacryloxypropyl trimethoxy silane; 0.5 wt% aq. solution.
[d] APS : Amino trimethoxy propyl silane; 0.5 wt% aq. solution.
[e] LiCA 38J : Neopentyl(diallyl)oxy, tri(dioctyl)pyro-phosphato titanate.

Table 3. The Effect of Various Conditions on IFSS the Microdroplet Test

various conditions	curing condition	IFSS(MPa)
pot time	10 min	12.4 (2.5)*
	120 min	10.1 (2.6)
diameter	14.7 μm	12.4 (2.5)
	30.3 μm	12.2 (2.0)
resin type	unsaturated polyester	12.4 (2.5)
	epoxy	29.3 (4.9)

* Standard deviation.
* Curing condition : 85 ℃ for 30 min.

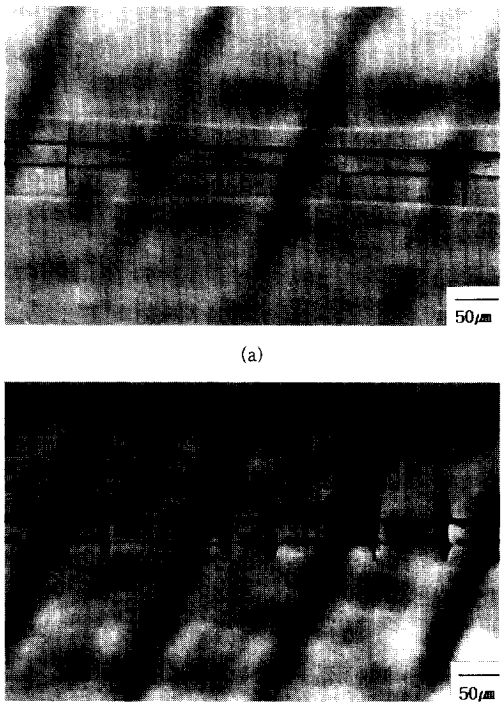

Figure 8. Optical micrographs of brittle unsaturated polyester matrix fragmentations in dual matrix composites : (a) The untreated and (b) VBAS 0.5 wt% treated cases.

in the interphase and flexibilized epoxy matrix.

Evaluation of the IFSS using Matrix Cracking Spacing. When a unidirectional, continuous fiber-reinforced composite is subjected to uniaxial tension, and if the fracture strain of the fiber is higher than that of matrix, then the

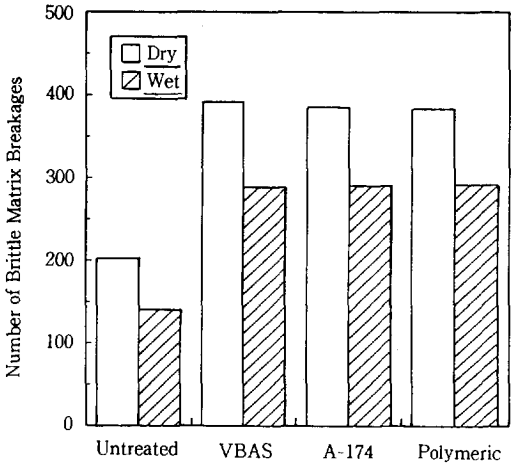

Figure 9. The number of brittle matrix breakage using various coupling agents in the dual matrix composites under dry and wet conditions.

first crack appears in the matrix. The crack is presumed to propagate through the matrix completely across the specimen normal to the fiber-stress axis, leaving the fibers bridging the crack.

According to the ACK model,[14] once a crack forms in the matrix, the matrix region adjacent to the crack is relieved of stress and thus further cracking is inhibited. The strain in the matrix increases with distance from the crack planes at a rate determined by the maximum frictional shear stress that can be developed by the interface until it again reaches the matrix strain-to-failure at a distance X from the crack. Cracking proceeds with no increase in load until there are approximately cracks normal to the fiber-stress axis spaced between X and $2X$ apart. This crack spacing, however, can be only expected when we assume a deterministic failure stress of matrix, and a single-valued interfacial stress, as shown in Fig. 10(a). The matrix crack spacing X is given by simple force balance, i.e., $2N\pi r_f \tau X = V_m \sigma_{mu}$ where N is the number of fiber per unit area, V_m the volume fraction of matrix, r_f fiber radius, σ_{mu} the stress at which the cracks begin to form, and τ is interfacial shear strength. Since $N = V_f/\pi r_f^2$ where V_f is the fiber volume fraction, X can be rewritten as follow:

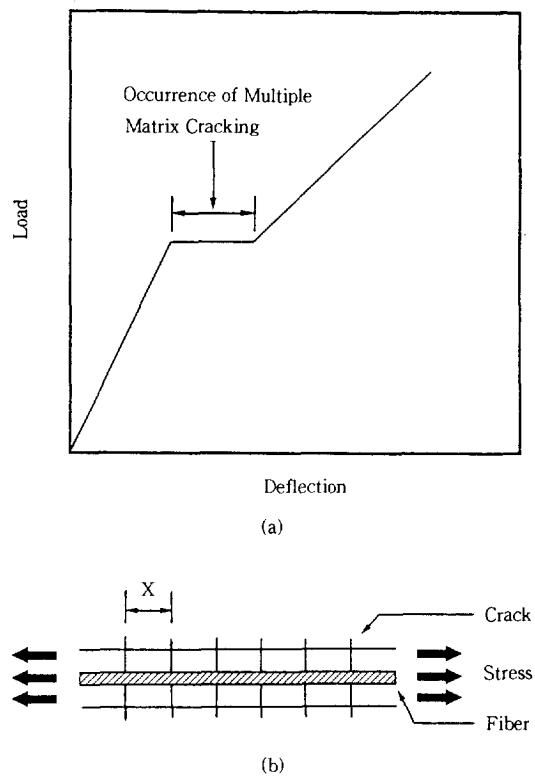

Figure 10. Schematic plot of the occurrence of multiple matrix cracking in ideal composite model during tensile test : (a) Plot of load versus deflection and (b) composite model.

$$X = (V_m/V_f)(\sigma_{mu} r_f/2\tau) \quad (2)$$

Eq. (2) was derived with assumption that the IFSS is constant, independent of the distance from the crack surface, and the matrix has a single-valued failure stress. The equation offers a mean by which the IFSS can be estimated from minimum matrix crack spacing, X, if the distribution of matrix crack spacing falls within a range X to $2X$. A deviation of crack spacing from the range of X to $2X$ has been explicitly

Table 4. Interfacial Shear Strength Evaluated Using Matrix Crack Spacing and Matrix Failure Stress

coupling agents	dry condition				wet condition			
	No. of matrix cracks	mean crack spacing (μm)	X (μm)	IFSS (MPa)	No. of matrix cracks	mean crack spacing (μm)	X (μm)	IFSS (MPa)
untreated	202.4 (19.2)	125.1 (19.2)	94.0 (8.3)	6.9 (0.7)	140.6 (9.4)*	181.4 (12.1)	135.6 (8.9)	4.8 (0.3)
polymer	383.6 (45.0)	66.2 (6.9)	49.5 (5.1)	13.1 (1.5)	291.8 (29.6)	87.0 (7.9)	65.0 (5.9)	10.0 (1.0)
VBAS	392.2 (38.6)	64.8 (5.8)	48.5 (4.4)	13.4 (1.3)	289.0 (22.8)	87.9 (6.4)	65.7 (4.8)	9.9 (0.8)
A-174	385.2 (26.2)	65.9 (4.2)	49.3 (3.1)	13.1 (0.9)	290.6 (12.5)	87.6 (3.8)	65.5 (2.8)	9.9 (0.5)

* Standard deviation.
* Values of V_f=0.3, V_m=0.7, σ_{mu}=37 MPa, r_f=15 μm were used in Eq. (2).
* Number of cracks within gauge length of 25.4 mm.
* Data obtained at least 6 sample were averaged.

described by Yang et al.,[15] using experimental evidence and computer simulation. Crack spacings were found to be distributed within X to 2 X with mean value of 1.337X only if the Weibull modulus (m) of matrix is infinitely large.

Applying the ideal of matrix crack spacing to the model system with a brittle matrix adjacent to the single glass fiber, an IFSS can be estimated and compared with the value obtained from the direct fiber pull-out test. Multiple matrix cracking occurred in brittle matrix as shown in Fig. 10(b) where the fiber treated with coupling agent exhibited about one half narrower crack spacing compared to the untreated fiber system.

From the configuration of a fiber with diameter of 30.3 μm and brittle matrix demonstrated in Fig. 10(b), V_f of about 0.3 was obtained. The matrix failure stress σ_{mu} of 37 MPa was measured by tensile test of brittle matrix alone. For more valid value of X, the number of matrix rack within the gauge length of 25.4 mm was counted and averaged using at least 6 specimens for each condition as given in Table 4. The system where the fiber treated with polymeric agent case yielded 383 cracks on average within 25.4 mm. Thus, average crack spacing is 66.3 μm. This in turn provides X value of 49.6 μm using the mean value of 1.337X as suggested by Yang. Applying these data to the Eq. (2), τ of 13 MPa for the polymer agent can be obtained. The IFSS of various systems evaluated using the same procedure were given in Table 4. A comparison of τ estimated from crack spacing with the value measured using fiber pull-out test shows that two values accord reasonably well while considering the standard deviation for the systems treated with various coupling agents, except the untreated.

Analysis of Acoustic Emission (AE). Fig. 11 showed the comparison of AE energy as a function of measuring time in three different type specimens. In Fig. 11(A) and (B), three groups were well separated in different ranges, whereas Fig. 11(C) showed only two distinct groups. Group (b) in Fig. 11(A) was the AE signals coming from brittle matrix cracking. The AE event numbers of group (b) in Fig. 11(B) were more than the number of Fig. 11(A) because of the effect of coupling agent.

Fig. 12 showed typical AE waveforms generated during tensile testing and their FFT results. The fiber breakage caused very large AE signals compared to the signals from brittle or ductile matrix failure. The AE waveform coming from fiber breakage appeared mainly about 100 kHz. The AE waveform from brittle matrix cracking was in the middle level and rel-

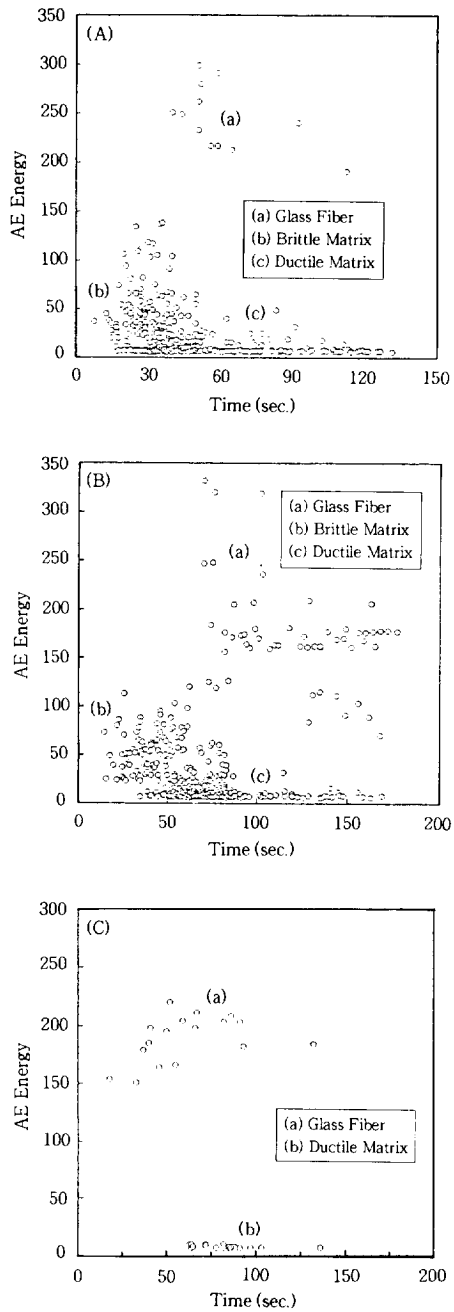

Figure 11. Comparison of AE energy as a function of measuring time in three different type specimens : (A) the untreated glass fiber/unsaturated polyester/epoxy, (B) the VBAS treated glass fiber/unsaturated polyester/epoxy, and (c) the untreated glass fiber/epoxy specimen.

atively small, whereas AE waveform from ductile matrix exhibited the smallest signal intensity among three failures. Characteristic peak of ductile matrix showed many noise signals due to low energy coming from ductile matrix fracture.

Brittle matrix fracture was observed by optical microscope and accompanying AE events were detected. AE method can be correlated successfully to the modified fragmentation technique in predicting the interfacial adhesion and the failure modes. These can suggest that AE method can be another technique to predict the failure modes and mechanisms in the dual matrix composites conveniently with the aid of micromechanical methods. Especially, it also can be applied in the ceramic matrix composites (CMC) where are in brittle and nontransparent matrices.

CONCLUSIONS

Tensile strength and elongation of glass fiber decreased with increasing gauge length due to a size effect coming from heterogeneous distribution of internal or external flaws in the fiber. The silane coupling agent treated glass fiber showed higher fiber strength than those of the untreated ones because of flaws healing. High concentrated case, however, the fiber strength decreases at higher concentration more than 2 wt% due to the stress concentration occurred at the lumpy coating region. In microdroplet test case, the IFSS was improved in the range of 20 to 35% when using silane coupling agents. This might be resulted from chemical and hydrogen bonding in two different interphases.

For modified fragmentation test, larger number of fragments occurred in brittle matrix layer were observed in the treated ones compared to the untreated composites under both dry and wet conditions. The relative interfacial adhesion

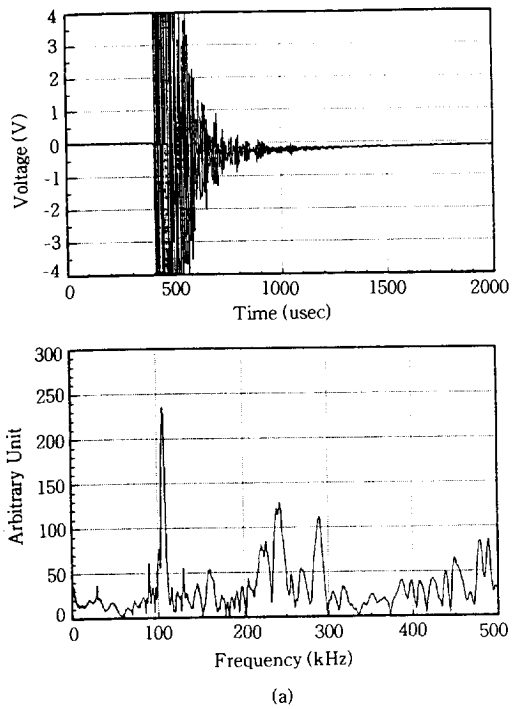

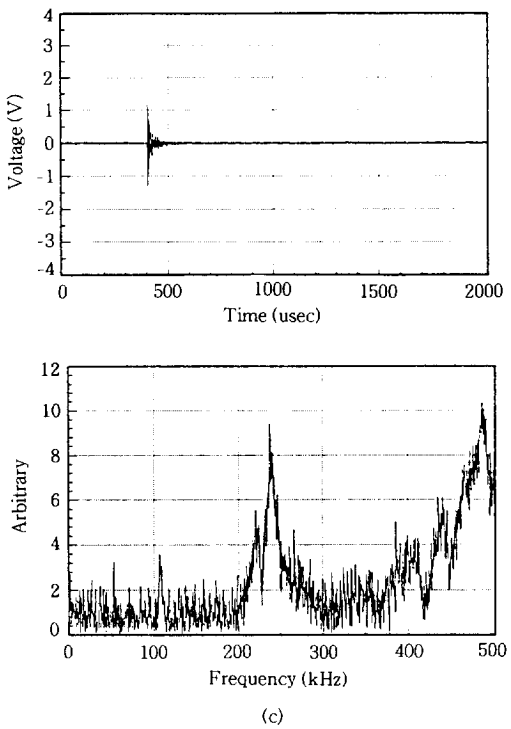

Figure 12. AE waveforms from dual matrices specimen while straining and their fast Fourier transfer (FFT) results : (a) fiber breakage, (b) brittle matrix cracking, and (c) ductile matrix cracking.

can be obtained from the number of fragments in brittle layer. The IFSS obtained from model methods accorded reasonably well with the experimental data predicted from pull−out test. There were three distinct AE distributions in dual matrix composites. AE waveforms and their FFT analysis provided the characteristic microfailure modes in the brittle layer cracking. Thus, AE method was useful in analysing the interfacial and microfailure properties of the composites consisting of nontransparent matrix.

Acknowledgement: This work was financially supported by Reserach Center for Aircraft Parts Technology (ReCAPT) of KOSEF.

REFERENCES

1. T. Grubb and Z. F. Li, *J. of Materials Science*, **29**, 189 (1994).
2. A. R. Sanadi and M. R. Piggott, *J. of Materials Science*, **20**, 431 (1985).
3. J. M. Park, R. V. Subramanian, and A. E. Bayoumi, *J. of Adhesion Sci. & Technol.*, **8**, 133 (1994).
4. J. M. Park, J. O. Lee, and T. W. Park, *Polymer Composites*, **17**, 375 (1996).
5. J. M. Park and R. V. Subramanian, *J. of Adhesion Sci. Technol.*, **5**, 459 (1991).
6. D. B. Marshall and W. C. Oliver, *Materials Science & Engineering*, **A126**, 95 (1990).
7. S. M. Lee and S. Holguin, *J. of Adhesion*, **31**, 91 (1990).
8. J. P. Favre and D. Jacques, *J. of Materials Science*, **25**, 1373 (1990).
9. D. Jacques and J. P. favre, *6th International Conf. on Composite Materials (ICCM)-V*, 471 (1987).
10. J. M. Park, S. I. Lee, E. M. Chong, W. K. Shin, D. J. Yoon, and J. H. Lee, *Polymer (Korea)*, **20**, 753 (1996).
11. B. T. Ma, L. S. Schadler, and C. Laird, *Polymer Composites*, **11**, 211 (1990).
12. R. K. Verma, R. G. Kander, and B. S. Hsiao, *J. of Materials Sci. Lett.*, **13**, 438 (1994).
13. L. Narisawa and H. Oba, *J. of Materials Science*, **19**, 1777 (1984).
14. J. Aveston, G. A. Cooper, and A. Kelly, *IPC Sci. and Technol. Press*, Guildford, U. K. 15 (1971).
15. X. F. Yang and K. M. Knowles, *J. Am. Ceram. Soc.*, **75**, 141 (1992).